Int J Clin Exp Pathol 2015;8(9):9796-9811
www.ijcep.com /ISSN:1936-2625/IJCEP0012967

Original Article

Up-regulation of AKAP13 and MAGT1 on cytoplasmic membrane in progressive hepatocellular carcinoma: a novel target for prognosis

Patamaporn Molee[1], Poom Adisakwattana[2], Onrapak Reamtong[3], Songsak Petmitr[3], Thaniya Sricharunrat[4], Nantana Suwandittakul[2], Urai Chaisri[1]

Departments of [1]Tropical Pathology, [2]Helminthology, [3]Molecular Tropical Medicine and Genetics, Faculty of Tropical Medicine, Mahidol University, Bangkok 10400, Thailand; [4]Pathology Unit, Chulabhorn Hospital, Bangkok 10210, Thailand

Received July 16, 2015; Accepted August 25, 2015; Epub September 1, 2015; Published September 15, 2015

Abstract: Hepatocellular carcinoma (HCC) is one of the most common cancers and is associated with high mortality worldwide. The current gold standards for HCC surveillance are detection of serum α-fetoprotein (AFP) and ultrasonography; however, non-specificity of AFP and ultrasonography has frequently been reported. Therefore, alternative tools, especially novel specific tumor markers, are required. In this study, cytoplasmic membrane proteins were isolated from phorbol 12-myristate 13-acetate (PMA)-induced invasive HepG2 cells and identified using nano-scale liquid chromatographic tandem mass spectrometry (NLC-MS/MS) with comparison to non-treated controls. The results showed that two proteins, magnesium transporter protein 1 (MAGT1) and A-kinase anchor protein 13 (AKAP13), were highly expressed in PMA-treated HepG2 cells. This up-regulation was confirmed by real-time RT-PCR, western blot analysis, and immunofluorescent staining studies. Furthermore, evaluation of MAGT1 and AKAP13 expression in clinical HCC tissues by immunohistochemistry suggested that both proteins were strongly expressed in tumor tissues with significantly higher average immunoreactive scores of Remmele and Stegner (IRS) than in non-tumor tissues ($P \leq 0.005$). In conclusion, the expression levels of MAGT1 and AKAP13 in HCC may be potential biomarkers for the diagnosis and prognosis of this cancer.

Keywords: Hepatocellular carcinoma, cytoplasmic membrane proteins, proteomics, MAGT1, AKAP13, immunohistochemistry

Introduction

Hepatocellular carcinoma (HCC) is a primary liver malignancy [1] that is the second most common cause of cancer deaths in men, and the sixth most common in women, worldwide [2]. Moreover, 80% of the burden is borne by countries in Asia and sub-Saharan Africa [3]. The incidence of HCC is reported to be highest in developing countries where infection with hepatitis B virus (HBV) is endemic.

At the present time, serum alpha-fetoprotein (AFP) levels greater than 400 ng/ml and ultrasonography performed every 6 to 12 months are the gold-standard techniques most commonly used for HCC detection. However, diagnosis of small HCC (≤ 3 cm in diameter) by detection of serum AFP levels and ultrasound is far from perfect [4, 5]. Therefore, identification and characterization of novel biomarkers is urgently needed for reliable diagnosis and prognosis of HCC.

Cytoplasmic membrane proteins are involved in central cellular processes such as cell signaling, cell-cell interactions, and ion and solute transport. Moreover, they seem to play an important role in several processes of cancer migration, invasion, and metastasis [6, 7]. Previous studies have used cytoplasmic membrane proteins for the diagnosis and prognosis of cancers. Human epidermal growth factor receptor 2 (Her2/neu) is a member of the epidermal growth factor family that plays an important role in the tumorigenesis of certain types

of breast cancer. Its over expression correlates with distinct diagnostic and therapeutic decisions [8]. In colorectal cancer (CRC), four cytoplasmic membrane proteins-tumor-associated calcium signal transducer 2 (TROP2, TACSTD2), transmembrane 9 superfamily member 2 (TM9SF2), tetraspanin-6 (TSPAN6), and tumor necrosis factor receptor superfamily member 16 (NGFR)-were evaluated with respect to improved diagnosis and treatment management. The results revealed that expression of all four proteins was markedly increased in the tumor compartment and associated with poor prognosis [9]. Caveolin-1 (Cav-1), an integral membrane protein, was shown to be over expressed in prostate cancer cells and related to progression of the disease [10]. In HCC, several cytoplasmic membrane proteins have been identified and characterized. MUC-1, a transmembrane mucin that is overexpressed in most cancers, showed increased expression during hepatocarcinogenesis and correlated with differentiation status [11]. Glypican-3 (GPC-3), an oncofetal protein and heparan sulfate proteoglycan, is anchored to the plasma membrane through glycosylphosphatidylinositol [12] and has been reported to be up-regulated in HCC [13]. However, an ideal cytoplasmic membrane protein for use as a tumor marker of HCC has not been identified.

In this regard, we identified cytoplasmic membrane proteins of invasive HCC for further development as effective diagnostic and prognostic tools. The HCC cell line HepG2 was treated with phorbol-12-myristate-13-acetate (PMA) to stimulate cancer cell invasion. PMA is a well-known selective activator of protein kinase C [14] and can act as a tumor promoter by inducing matrix metalloproteinase-9 (MMP-9) expression in certain cancer cells [15]. Weng and colleagues found that PMA induced MMP-9 expression in HepG2 cells together with strongly stimulated phosphorylation of ERK1/2 and slightly stimulated phosphorylation of Akt, and contributed to the cell invasion ability of HepG2 cells [16]. After treatment with PMA, cytoplasmic membrane proteins were isolated and verified by nano-scale liquid chromatographic tandem mass spectrometry (NLC-MS/MS). Candidate proteins were selected and validated with real-time PCR, western blotting, and immunofluorescent staining. Finally, expression of selected candidate proteins in clinical HCC tissues was determined and graded compared with normal surrounding tissue. The results of these studies may lead to more reliable diagnosis and prognosis of HCC in the future.

Materials and methods

Culture of hepatocellular carcinoma cell line

Human hepatoma cells (HepG2 cell line, kindly gifted by Dr. Jetsumon Prachumsri, Mahidol Vivax Research Center, Faculty of Tropical Medicine, Mahidol University, Thailand) were grown in HyClone™ Dulbecco's modified Eagle's medium (DMEM; GE Healthcare, Logan, UT, USA), supplemented with 10% (vol/vol) fetal bovine serum (Biowest, Nuaillé, France), 1 × penicillin/streptomycin (Biowest), and 0.37% (wt/vol) $NaHCO_3$ at 37°C in a humidified atmosphere of 95% air and 5% CO_2.

MTT assay

The cytotoxic effects of phorbol 12-myristate 13-acetate (PMA; Sigma-Aldrich, St Louis, MO, USA) on HepG2 cells were determined by measurement of cell proliferation using the MTT (3-[4,5-dimethylthiazolyl-2]-2,5-diphenyltetrazolium bromide, a yellow tetrazole) assay as previously described with some modifications [17]. Briefly, 100 ml of HepG2 cells (7.5×10^4 cells/ml) were seeded into 96-well culture plates (Corning Inc., Corning, NY, USA) and incubated at 37°C for 16-18 h under 5% CO_2 before addition of PMA (Sigma-Aldrich) at different concentrations (0, 1, 10, 100, 1,000, and 2,000 nM). After incubation for a further 16-18 h, 40 µl of 5 mg/ml MTT was added to each well, including one set of wells containing MTT but no cells as a control. The cells were incubated under dark conditions for 3.5 h at 37°C, and then 150 µl of DMSO (Amresco, Solon, OH, USA) was added and the plate was gently shaken for 15 min. Optical density was measured at a wavelength of 595 nm with an ELISA reader (Tecan, Switzerland). This study was performed in triplicate in three independent experiments.

Cell invasion assay

A transwell invasion assay was performed to determine the effect of PMA on invasion of HepG2 cells as described previously [18]. In brief, membranes of 24-well transwell plates

(Corning Inc.) were coated with 100 μl of a 1 mg/ml solution of matrigel (Becton-Dickinson, NJ, USA) and incubated at 37°C for 4-5 h for gelling. Next, 100 μl of HepG2 cells (1×10^6 cells/ml) was applied to the upper chamber and PMA was added at a final concentration of 100, 200, and 500 nM. The lower chamber was filled with 650 μl of DMEM supplemented with 1% fetal bovine serum. The plates were incubated at 37°C for 24 h. For time-dependence studies, the PMA concentration that induced the greatest level of HepG2 invasion was chosen and the number of invading cells was determined at 24, 36, and 48 h. To determine cell invasion, the membranes were stained with Giemsa (Sigma, St. Louis, MO, USA) and invading cells on the lower side of the membrane were counted under a light micros cope (Olympus BX41; USA). The results were expressed as mean ± standard deviation (S.D.) of duplicate assays performed in identical conditions.

Cell membrane preparation

Cytoplasmic membrane proteins of PMA-induced and non-induced HepG2 cells were isolated using a cell surface protein isolation kit (Thermo Scientific, Waltham, MA, USA) according to the manufacturer's instructions. Briefly, HepG2 cells were incubated with or without 200 nM PMA at 37°C for 24 h and then cytoplasmic membrane proteins were labeled with EZ-LinkSulfo-NHS-SS-Biotin, a thiol-cleavable amine-reactive biotinylation reagent (GE Healthcare, UK). After lysing cells with a mild detergent, the labeled proteins were isolated with immobilized neutravidin gel (agarose beads; GE Healthcare) and bound proteins were subsequently released by incubation with SDS-PAGE sample buffer containing 50 mM DTT (GE Healthcare).

Proteomic analysis

Cytoplasmic membrane proteins from PMA-induced and non-induced HepG2 cells were separated by 12% SDS-PAGE (80 mm × 680 mm × 60.75 mm; Hoefer® Systems; MA, USA). The gels were stained with Coomassie Brilliant Blue G250 solution (Bio-Rad, Hercules, CA, USA) and each protein lane was excised in 20 rectangles (**Figure 1**). The gels were destained with destaining solution [50 mM NH_4HCO_3, 50% (V/V) acetonitrile (ACN)], reduced with 5 mM dithiothreitol (DTT) (GE Healthcare, UK), and alkylated with 250 mM iodoacetamide (IAM; GE Healthcare, UK). The gel pieces were incubated in the dark for 30 min and then dehydrated with 200 ml ACN. Proteins in gels were digested to peptides by incubation with trypsin (100 ng/ml; Sigma) at 37°C overnight. Peptides were extracted from the gels with 50% (V/V) ACN, dried by vacuum evaporator (Labconco, Kansas City, MO, USA) and resuspended with 0.1% formic acid. Each peptide suspension was subjected to an Ultimate 3000 nano-LC system (Dionex; Surrey, UK) coupled with tandem mass spectrometry (NLC-MS/MS; micrOTOF-Q II, Bruker; Bremen, Germany) and the mass spectra were processed using analysis software (DataAnalysisTM 4.0, Bruker) according to a previous publication [19]. Mascot version 2.4.1 (Matrix Science, London, UK) was used to search the .mgf file against the SwissProt database Homo sapiens was set as the taxonomy filter. Missed cleavage was set to 1. Variable modification was set to cysteine carbamidomethylation and methionine oxidation. Protein expression profiles from PMA-treated and non-treated experiments were compared by the exponentially modified protein abundance index (emPAI) ratio [20]. All reported emPAI values in this research were the mean of three MS analysis replications. Only protein hits from the MASCOT search with 95% confidence were demonstrated. Cytoplasmic membrane proteins that showed greater than 2-fold up-regulation in PMA-treated HepG2 cells were selected for further validation.

SYBR real-time RT-PCR for analysis of gene expression

Total RNA of PMA-treated and non-treated HepG2 cells was extracted using Ribozol™ reagent (Amresco) according to the manufacturer's instructions and 5 μg aliquots of RNA were treated with DNase I (Thermo) to eliminate contaminating genomic DNA. First-strand cDNA was prepared from 1 μg of DNA-free RNA using a first strand construction kit (Thermo) according to the manufacturer's instructions. The level of gene expression was determined by SYBR real-time polymerase chain reaction (SYBR real-time RT-PCR) in a total volume of 20 μl containing 3.2 μl cDNA, 100 nM forward primer, 100 nM reverse primer, and 1 × SsoAdvanced™ SYBR® Green Supermix (Bio-Rad). The reaction was performed at 95°C for 3

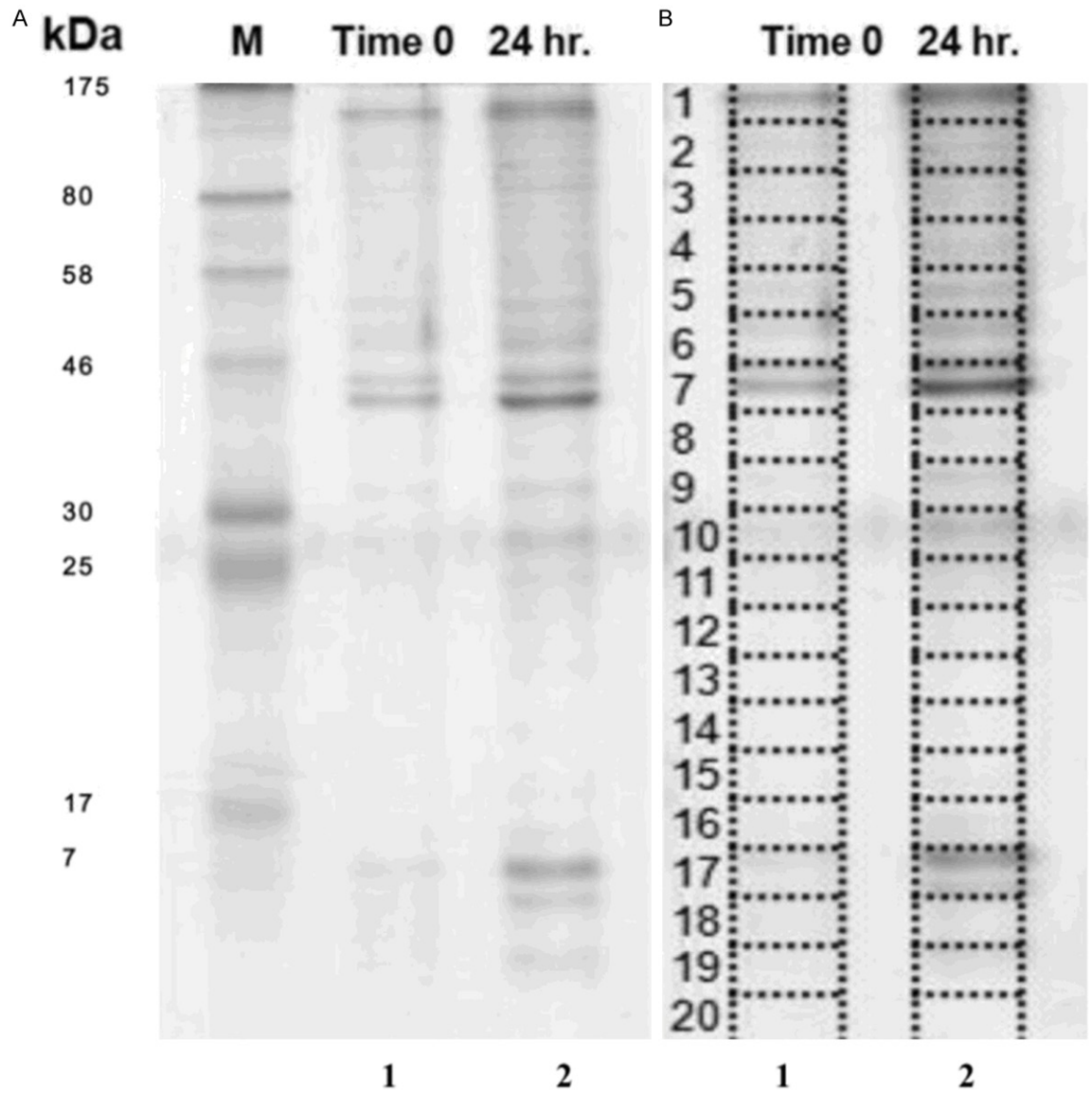

Figure 1. Separation of enriched cytoplasmic membrane proteins by 12% SDS-PAGE.

min followed by 45 cycles of 95°C for 30 s and 60°C for 10 s using a LightCycler® 480 II Real-Time PCR System (Roche Diagnostics, Roche Applied Science, Germany). Specific primers for amplification of gene targets were designed using the Primer3 program (http://frodo.wi.mit.edu/primer3/). The primers used for specific gene targets and the housekeeping gene, glyceraldehyde 3-phosphate dehydrogenase (*GAPDH*), are shown in **Table 1**.

SYBR real-time RT-PCR was performed in triplicate in two independent experiments. The level of target gene expression was calculated with normalization to *GAPDH* using the formula of $2^{-\Delta Cp}$. The fold change in transcription was calculated by comparison of PMA-treated and non-treated HepG2 cells using the formula of $2^{-\Delta\Delta Cp}$ [21].

Western blot analysis

Based on data from mass spectrometry and SYBR real-time RT-PCR, two interesting proteins, AKAP13 and MAGT1, were selected for further validation. For western blot analysis, PMA-treated and non-treated HepG2 cells were lysed with RIPA buffer and protein concentration was measured using the Pierce™ Coomassie (Bradford) Protein Assay Kit

Table 1. Primers used for real-time RT-PCR analysis of gene expression profile in HepG2 cells

No.	Gene	Accession no.	Product size (bp)	Primers (5'-3')	Primer length (nt)
1	*hSTOM*	NM004099	199	5' CGTTCTCATTCTTATTCACCGTTAT 3'	25
				5' TCAAATGAAATAGTTCTCATGTCCA 3'	25
2	*hGTR1*	P11166	249	5' GGGATCAATGCTGTGTTCTATTACT 3'	25
				5' ACAGACAAAGCTCATCCCATTATAG 3'	25
3	*hACTN1*	NM001102	249	5' CAACATCCAGAACTTCCACATAAG 3'	24
				5' TGGTAGAAGCTAGACACGTAAGTCA 3'	25
4	*hMAGT1*	Q9H0U3	121	5' TGAAACACACATTGTTCTTCTGTTT 3'	25
				5' AATACCAGCCACACACATTATCTTT 3'	25
5	*hSTML3*	Q8TAV4	202	5' CTCCGTAACTACTCAGGTAGATGGA 3'	25
				5' ATCAAGTAAAGTCTGGATGCTATGG 3'	25
6	*hAKAP13*	Q12802	222	5' GAGAGTGTACCTCAAAACAAGGTGT 3'	25
				5' TTAAAATCTGGGAGAGAGACACATC 3'	25
7	*hCAMP3*	Q9P1Y5	183	5' CATTCTGGAGGAAATTGAGAAAAG 3'	24
				5' GAGTTGTACTTGTAGATGCCTTCCA 3'	25

(Thermo Fisher Scientific Inc.) according to the manufacturer's instructions. The cell lysates were separated by 12% SDS-PAGE and transferred to a polyvinylidene fluoride (PVDF) membrane (Pall Corporation, Port Washington, NY, USA). The blotting procedure was performed as described previously [19] with some modifications. In brief, membranes were blocked with 5% skimmed milk and then incubated with mouse-monoclonal anti-human AKAP13 (N-terminal) antibody (Sigma-Aldrich), rabbit anti-human MAGT1 antibody (Sigma-Aldrich), or mouse anti-human β-actin antibody (Cell Signaling Technology, Beverly, MA, USA). After washing, the membrane was incubated with goat anti-mouse IgG (H + L) (Southern Biotech, Birmingham, AL, USA) or goat anti-rabbit *Ig*G (H + L) conjugated with horseradish peroxidase (Southern Biotech) secondary antibodies. The signal was developed using Super Signal™ West Dura Extended Duration chemiluminescence substrate (Thermo Fisher Scientific Inc.) and detected by Image Quant™ LAS 4000 (GE Healthcare). Protein band intensity was analyzed using the ImageJ program (http://imagej.nih.gov/ij/) and normalized to that of β-actin. The normalized intensity of the target proteins in PMA-treated and non-treated HepG2 was compared and fold change was calculated. The experiment was performed in triplicate.

Immunofluorescence

Five hundred microliters of HepG2 cells in complete medium (2×10^6 cells/ml) was seeded into 24-well culture plates (Nunc™, Thermo) containing a 1.5-cm diameter sterile glass cover slip (Thermo) and incubated at 37°C and 5% CO_2 for 24 h prior to treatment with 200 nM PMA and incubation for a further 24 h. Non-treated HepG2 cells were processed in parallel as a control. After incubation, the coverslips were removed, washed thoroughly with 1 × PBS and blocked with blocking solution (3% FBS in 1 × PBS) at room temperature for 1 h. The coverslips were rinsed with 1 × PBS three times for 5 min each and incubated with mouse anti-human AKAP13 antibody (1:200; Sigma-Aldrich) or rabbit anti-human MAGT1 (N-terminal) antibody (1:500; Sigma-Aldrich) in blocking solution at room temperature for 2 h. After washing 3 times with 1 × PBS, the coverslips were incubated with Cy3-donkey anti-rabbit IgG minimal X-reactivity antibody (1:500; Biolegend, San Diego, CA, USA) and FITC-goat anti-mouse IgG minimal X-reactivity antibody (1:500; Biolegend) at room temperature for 1 h. The coverslips were washed with 1 × PBS three times for 5 min each and mounted with 50% glycerol. Digital images were acquired using a fluorescence microscope (Olympus BX41 and Olympus DP20; Olympus, Tokyo, Japan) and DP2-B2W-E-V2.2 software (Germany).

Immunohistochemical staining and semi-quantitative analysis

Clinical samples from 10 patients (7 male, 3 female) with histopathologic diagnosis of HCC were kindly provided by the Pathology Unit of

Table 2. Clinicopathologic data of patients with hepatocellular carcinoma

No.	Age (years)	Sex	Tumor grade	TNM staging of tumor/ tumor stage	Hepatitis infection
1	65	M	3	$T_2N_0M_0$/Stage II	HBV
2	51	M	3	$T_2N_0M_0$/Stage II	HBV
3	45	M	3	$T_2N_0M_0$/Stage II	HBV
4	66	M	3	$T_1N_xM_0$/Stage I	HBV
5	67	M	1 and 2	$T_2N_xM_0$/Stage II	HBV
6	60	M	2	$T_2N_xM_0$/Stage II	HBV, HCV
7	78	M	3	$T_2N_xM_0$/Stage II	HBV
8	72	F	3	$T_{3a}N_0M_0$/Stage IIIA	Others
9	57	F	3	$T_2N_xM_0$/Stage II	HBV
10	62	F	3	$T_1N_0M_0$/Stage I	HCV

Chulabhorn Hospital, Thailand. All samples were categorized as leftover specimens with ethical approval of both the Faculty of Tropical Medicine (TMEC 13-031) and Chulabhorn Hospital (14/2557). The case records of the patients are shown in **Table 2**.

Expression of AKAP13 and MAGT1 in HCC patient tissues was determined to confirm our findings in the HepG2 cell line. Paraffin-embedded sections (4-μm thickness) were processed as described elsewhere [22] before incubation with antibodies. After blocking (Protein block, Mouse and Rabbit Specific HRP/DAB [ABC] Detection IHC kit, Abcam), 200 μl of 1:25 dilution of mouse anti-human AKAP13 (N-terminal) antibody (Sigma-Aldrich) or 1:25 dilution of rabbit anti-human MAGT1 antibody (Sigma-Aldrich) was applied and the sections were incubated at room temperature for 16-18 h. After washing to remove the primary antibody, the sections were incubated sequentially with biotinylated goat anti-polyvalent antibody and streptavidin peroxidase (Mouse and Rabbit Specific HRP/DAB [ABC] Detection IHC kit, Abcam) at room temperature for 10 min each. The secondary antibodies were removed by washing with 1 × PBS and color was developed using the HRP/DAB (ABC) Detection IHC kit (Abcam) according to the manufacturer's instructions. Ready-to-use Mayer's Hematoxylin solution (Biomol GmbH, Germany) was used for counterstaining. The sections were dehydrated by sequential incubation with 95% ethanol (two changes), 100% ethanol (two changes), and xylene (three changes) and then mounted with a coverslip in mounting medium (Thermo Fisher Scientific Inc.).

Semi-quantitative analysis was performed by comparing the number of AKAP13-positive and MAGT1-positive cells in tumor tissue with that in non-tumorous surrounding tissue. The procedure and scoring were performed according to a previous publication [23]. All tissues were examined under at least 10 high-power fields in a standardized manner by three professional examiners.

Statistical analysis

Invasion assay data and gene expression profiles between PMA-treated and non-treated HepG2 were statistically analyzed by non-parametric *t*-test with a p value ≤ 0.05 considered significant. Significant differences in western blot data among cell lines were determined by one-way ANOVA at $P \leq 0.05$. The IRS scoring of immunohistochemistry for the HCC tissues and corresponding non-tumor tissues were statistically analyzed by multiple *t* test with a p value of ≤ 0.005, with multiple comparisons performed using the Holm-Sidak method for positivity (negative, weak, mild, and strong). All results represent the mean ± SD of triplicate determinations. Correlation analysis of all experiments was performed with Graphpad Prism6 software (La Jolla, CA, USA).

Results

Effect of PMA on proliferation and invasion of HepG2 cell line

A previous study reported that PMA could activate the proliferation and invasion of HepG2 cells [16]. We repeated this experiment to optimize the concentration of PMA for further experiments. An increasing concentration of PMA (0.1, 1, 10, and 100 nM) progressively induced HepG2 cell proliferation compared with non-treated controls (data not shown). However, a very high concentration of PMA (1,000 and 2,000 nM) inhibited HepG2 cell proliferation (data not shown).

From the results reported above, a PMA concentration range of 100-500 nM was selected and its effect on invasion of HepG2 cells was

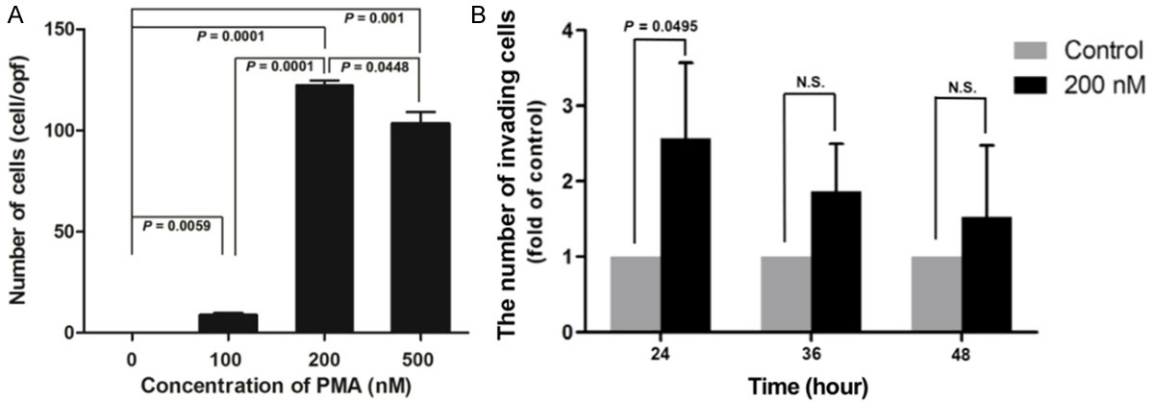

Figure 2. PMA stimulated invasiveness of HepG2 cells in a dose-dependent (A) and time-dependent (B) manner. Time-dependent analysis was performed by treating HepG2 cells with 200 nM PMA for different durations.

Table 3. Up-regulated cytoplasmic membrane proteins in PMA-induced and non-induced HepG2 cells

Accession	Protein	Sub cellular location	Mass	pI	emPAI value	
					Non PMA induction	PMA induction
STOM-HUMAN	Erythrocyte band 7 integral membrane protein	Cell membrane	12651	5.92	ND	1.45 ± 0.14
GTR1-HUMAN	Solute carrier family 2, facilitated glucose transporter member 1	Cell membrane	56157	7.79	ND	0.07 ± 0.02
ACTN1-HUMAN	Alpha-actinin-1	Cell membrane	97980	9.75	ND	0.07 ± 0.01
MAGT1-HUMAN	Magnesium transporter protein 1	Cell membrane	41689	4.76	ND	0.10 ± 0.03
STML3-HUMAN	Stomatin-like protein 3	Cell membrane	30291	5.75	ND	0.12 ± 0.02
AKAP13-HUMAN	A-kinase anchoring protein 13	Cell membrane	25740	7.82	ND	0.01 ± 0.00
CAMP3-HUMAN	Calmodulin-regulated spectrin-associated protein 3	Cell membrane	37464	5.98	ND	0.03 ± 0.01

N = 3, "ND" represents "Not detected".

monitored using a matrigel invasion assay. The number of invaded cells in the presence of 200 nM PMA was significantly higher compared with other concentrations of PMA as well as the non-treated control (**Figure 2A**). The optimal time was determined by treatment of HepG2 cells with 200 nM PMA and monitoring cell invasion at 0, 24, 36, and 48 h. The results suggested that the highest number of invaded HepG2 cells was achieved at 24 h (P = 0.0495); additional incubation for 36 and 48 h progressively decreased cell invasion compared with 24 h (**Figure 2B**).

Up-regulation of cytoplasmic membrane proteins on invading HepG2 cells

Based on the above data, HepG2 cells were treated with 200 mM PMA for 24 h before preparation of cytoplasmic membrane proteins. Non-treated HepG2 cells were processed in parallel as a control. Cytoplasmic membrane proteins isolated from PMA-treated and non-treated cells were separated by 12% SDS-PAGE and each lane was excised as small rectangles prior to mass spectrometry analysis (**Figure 2**). The results from NLC-MS/MS of membrane fraction incorporating the Mascot search identified up to 300 proteins, of which seven cytoplasmic membrane proteins were detected only in PMA-treated cells. The list of proteins with relevant information is summarized in **Table 3**. The criteria used to select the candidate proteins were as follows: (1) up-regulation greater than 2 fold compared with non-treated control, (2) present in PMA-treated HepG2 but not in control, (3) no or little available information regarding role in HCC development.

Expression level of novel candidate cytoplasmic membrane proteins in PMA-treated HepG2 cells

SYBR real-time RT-PCR was performed to determine gene expression of all 7 candidate proteins in PMA-treated and non-treated HepG2 cells. *MAGT1* and *AKAP13* were highly expressed in PMA-treated cells compared with

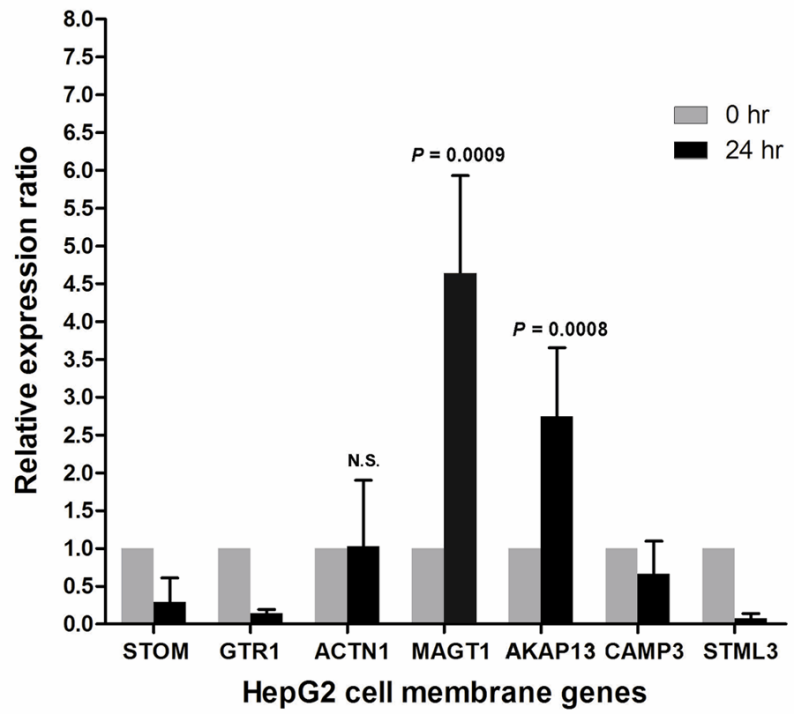

Figure 3. Analysis of gene expression by SYBR green real-time PCR. Among seven candidate mRNAs, *MAGT1* and *AKAP13* were significantly up regulated at 24 h in PMA-treated HepG2 cells compared with non-treated cells (0 h) as determined by t-test ($P \leq 0.05$). The relative expression levels of *STOM*, *GTR1*, *ACTN1*, *MAGT1*, *AKAP13*, *CAMP3*, and *STML3* mRNA were 0.29, 0.15, 1.03, 4.64, 2.74, 0.66 and 0.07, respectively.

non-treated controls with a fold change unit of 4.64 ($P = 0.0009$) and 2.74 ($P = 0.0008$), respectively (**Figure 3**). These results supported the protein expression levels determined by mass spectrometry. However, the other candidates, erythrocyte band 7 integral membrane protein (*STOM*), solute carrier family 2, facilitated glucose transporter member 1 (*GTR1*), alpha-actinin-1 (*ACTN1*), stomatin-like protein 3 (*STML3*), and calmodulin-regulated spectrin-associated protein 3 (*CAMP3*), yielded controversial results for mRNA expression compared with mass spectrometry results. Therefore, only MAGT1 and AKAP13 were selected for further analysis by Western blotting.

Expression of MAGT1 and AKAP13 protein in PMA-treated HepG2 cells at 0, 6, 12, 24, and 48 h were determined by western blot analysis. Expression of both proteins increased in a time-dependent manner, with the highest expression level (approximately 4-fold higher than in the non-treated control) observed at 24 h. Prolonged incubation for 48 h did not further increase the protein level but rather decreased it, as shown in **Figure 4**.

High-intensity localization of MAGT1 and AKAP13 at the cytoplasmic membrane of PMA-induced HepG2 cells

Expression intensity and location of MAGT1 and AKAP13 were investigated using an immunofluorescent staining technique. The results showed that MAGT1 and AKAP13 were expressed at the membrane and in perimembranous areas of PMA-treated HepG2 cells and at higher levels than in non-treated controls (**Figure 5**). This localization may indicate roles of both MAGT1 and AKAP13 in biologic and physiologic processes of cell invasion.

Detection of MAGT1 and AKAP13 expression in clinical hepatocellular carcinoma samples

Clinical HCC samples were stained with antibodies against human MAGT1 or AKAP13 and signal was developed using a colorimetric substrate. The pattern and intensity of protein expression were observed and graded according to the IRS scoring system. MAGT1 was detected in the cytoplasm of all cases of HCC but not in the non-tumoral surrounding tissue ($P \leq 0.005$) (**Figure 6**). Similarly, AKAP13 was highly expressed in the cytoplasm of HCC cells but was undetectable in normal tissue ($P \leq 0.005$) (**Figure 7**).

Comparison of average IRS score and intensity of MAGT1 and AKAP13 expression in tumor tissues with that in non-tumoral surrounding tissue showed that both values were significantly higher in HCC tissue than in non-tumor tissue (**Figure 8A** and **8B**).

Discussion

The annual prevalence and incidence of HCC remains high worldwide, and especially in developing countries. Although standard diag-

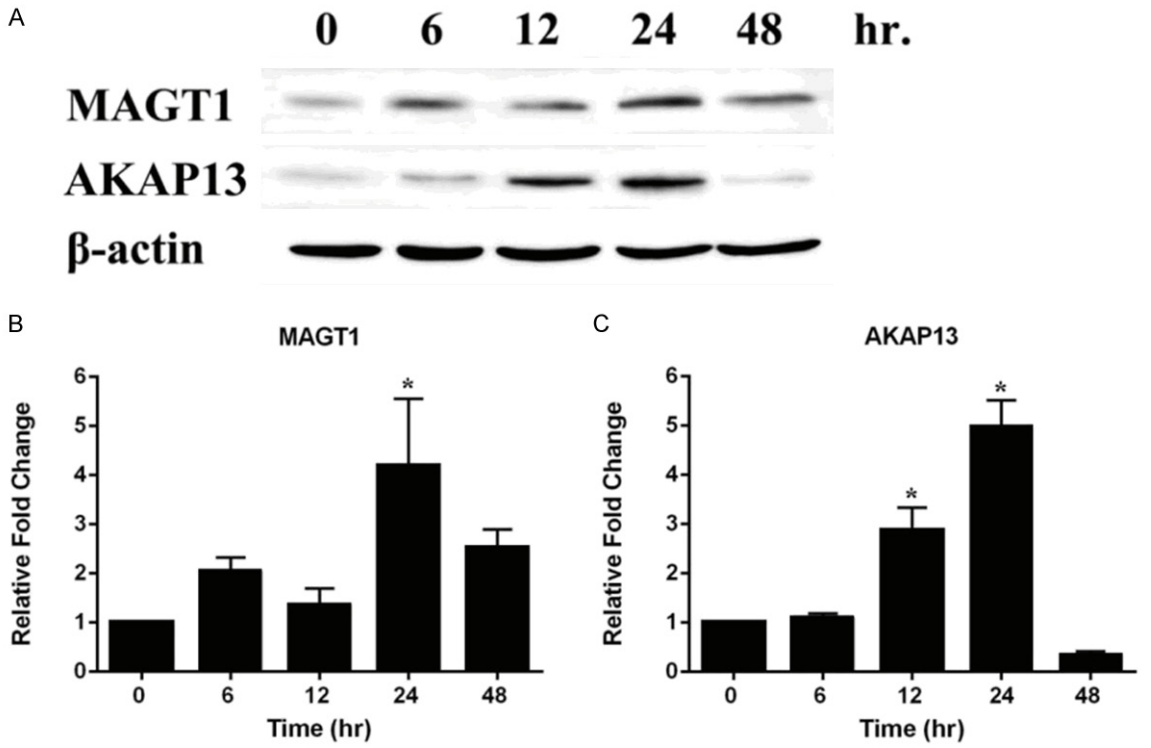

Figure 4. Expression of MAGT1 and AKAP13 protein at 0, 6, 12, 24, and 48 h in PMA-treated HepG2 cells. (A) Representative immunoblot. (B and C) Individual data were quantified as intensity normalized to β-actin expression. Data were expressed as relative fold change and presented as mean ± SD of three independent experiments, $*P \leq 0.05$, compared with the 0 h time point.

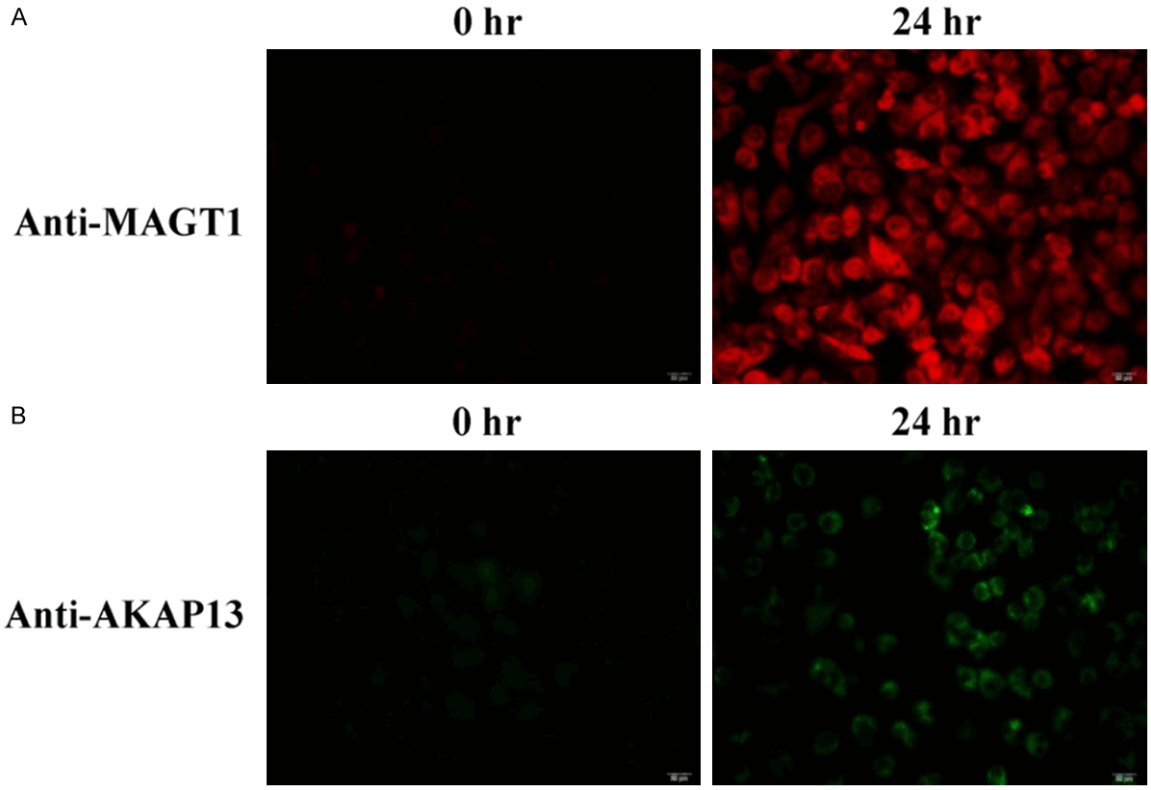

Figure 5. Immunolocalization of MAGT1 and AKAP13 in HepG2 cells. (A) Representative photomicrographs showing increased red fluorescence of MAGT1 localization in PMA-treated HepG2 cells at 24 h (right panel) compared with 0 h (left panel). (B) Representative photomicrographs showing increased green fluorescence intensity of AKAP13 localization in PMA-treated HepG2 cells at 24 h (right panel) compared with 0 h (left panel) (magnification × 40).

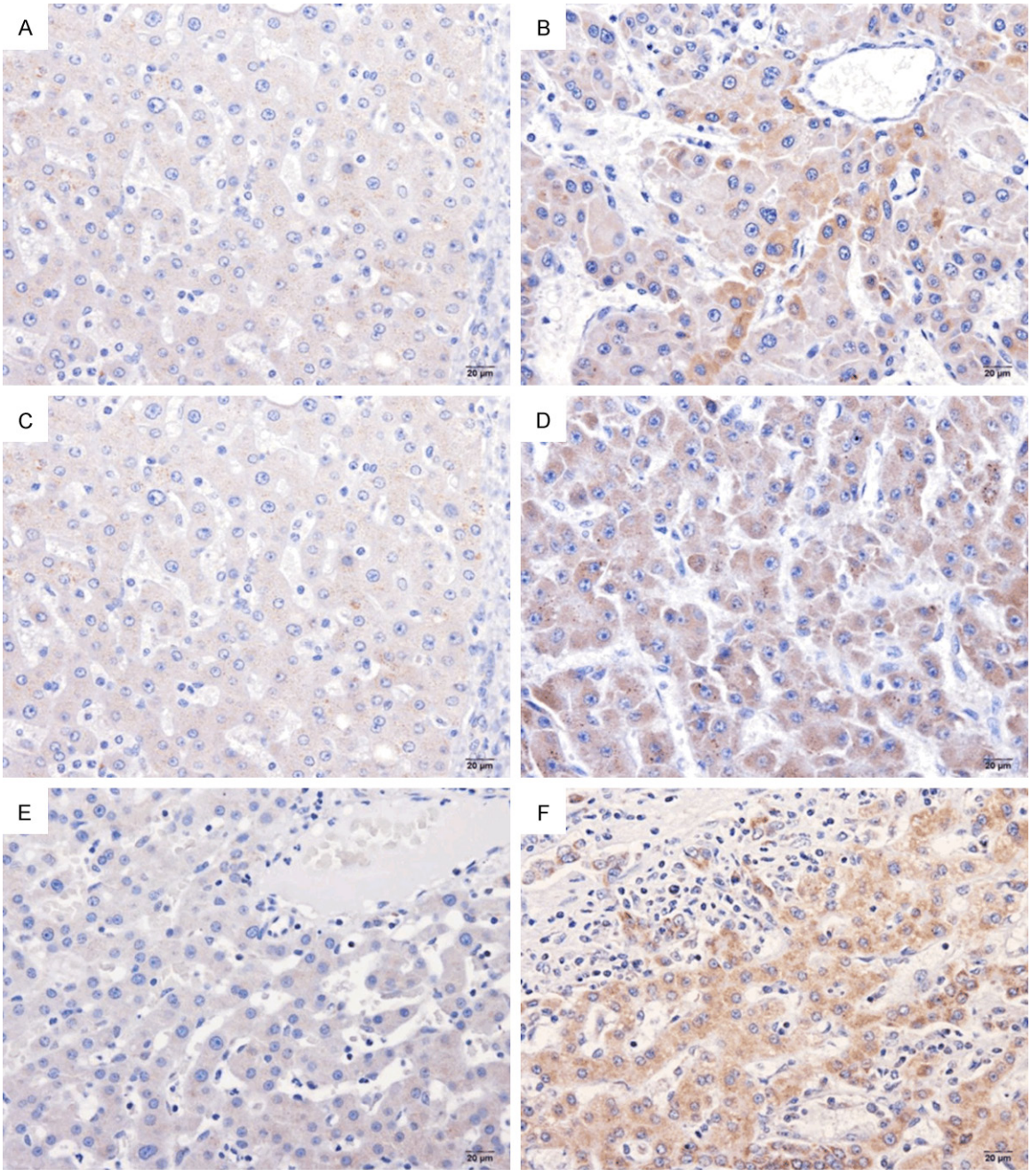

Figure 6. Immunohistochemical staining of MAGT1 in liver tissues of three patients with HCC of each grade. MAGT1 staining was not observed in the cytoplasm of normal hepatocytes of non-tumoral surrounding tissues (A, C, E) but was positive in the cytoplasm of tumor cells of all three patients (B, D, F). (Grade 1; A and B, Grade 2; C and D, Grade 3; E and F; magnification × 40).

nostic surveillance techniques, such as serum AFP and ultrasonography, are commonly available with affordable cost misdiagnosis associated with poor prognostic markers has been a

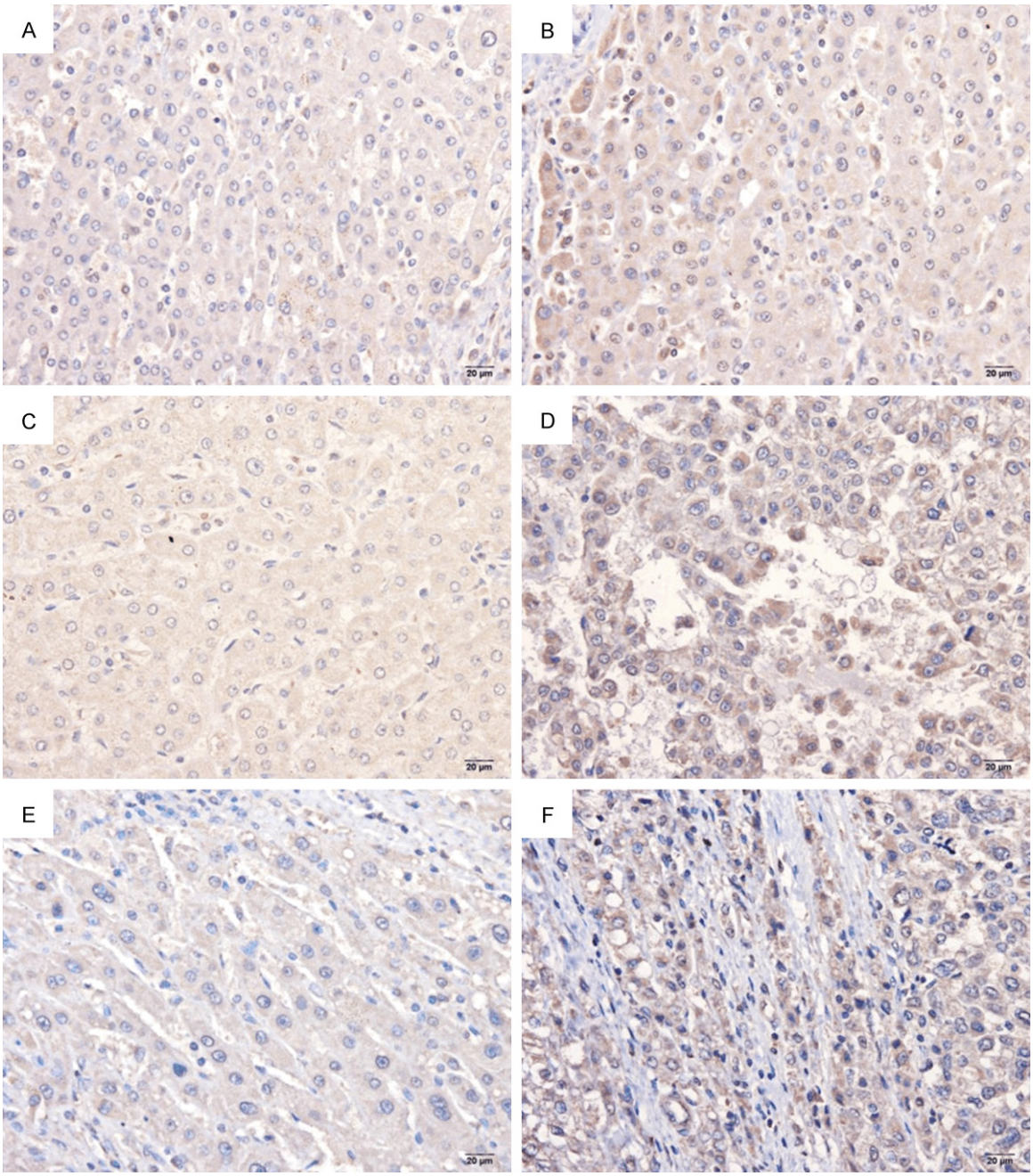

Figure 7. Immunohistochemical staining of AKAP13 in liver tissues of three patients with HCC of each grade. The brown particles were distributed in the cytoplasm of tumor cells from all three patients (B, D, F). However, a yellow or brown precipitation could not be detected in the non-tumoral surrounding tissues (A, C, E). (Grade 1; A and B, Grade 2; C and D, Grade 3; E and F; magnification × 40).

problem for several decades [24, 25]. Identification of novel tumor markers, specifically cytoplasmic membrane proteins, may lead to reliable diagnosis and prognosis for HCC in the near future. In this study, mass spectrometry was applied to identify cytoplasmic membrane proteins expressed by the invasive HCC cell line HepG2. Treatment of HepG2 cells with 200 nM PMA for 24 h facilitated cell proliferation and invasion, consistent with the previous report by Weng *et al.* [16]. PMA is a well-known tumor promoter that induces expression of MMP-9 during the invasion and metastasis of various tumor cells [26].

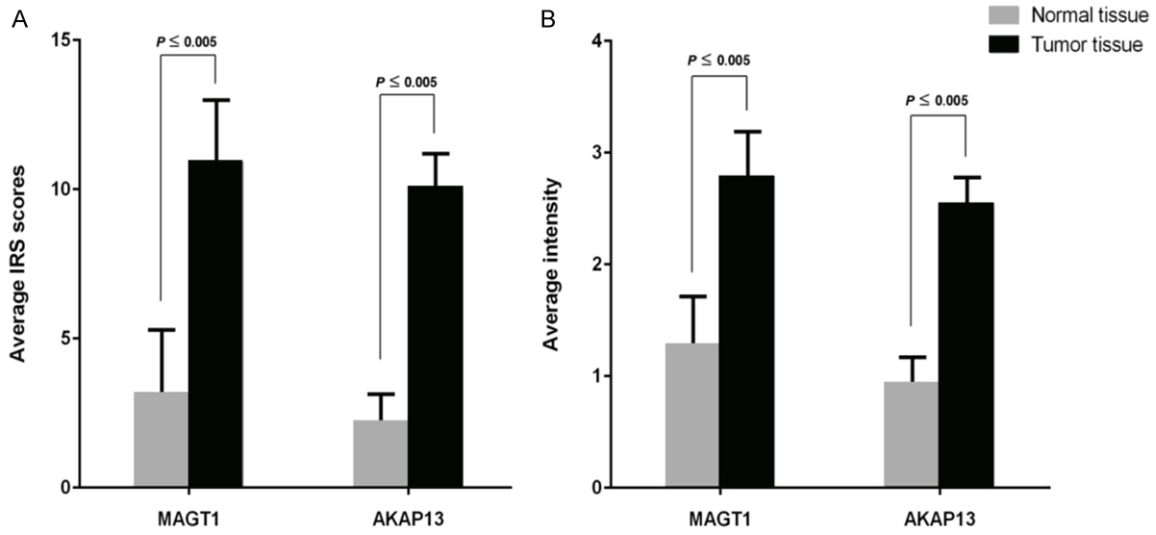

Figure 8. Average IRS score (A) and intensity (B) of non-tumor tissues compared with tumor tissues. According to IRS values, IRS ≥ 1 is positive expression, whereas IRS < 1 is negative expression. The average IRS score of MAGT1 protein in human HCC tissues was moderately to strongly positive compared with negative to moderate IRS scores in non-tumor tissues ($P \leq 0.005$). The IRS score of AKAP13 protein showed strongly positive expression in human HCC tissues compared with negative to mild IRS scores in non-tumoral surrounding tissues ($P \leq 0.005$). The average intensity of immunostaining in non-tumor tissues was 1.287 for MAGT1 and 0.917 for AKAP13, compared with 2.79 and 2.55, respectively in tumor tissues. Both MAGT1 and AKAP13 showed significantly higher average IRS scores and intensity of immunostaining in tumor tissues compared with non-tumor tissues ($*P \leq 0.005$) (IRS: Immunoreactive *score* of Remmele and Stegner).

Use of mass spectrometry to identify cytoplasmic membrane proteins of PMA-induced invading HepG2 cells indicated that seven predominant proteins were expressed only in response to PMA. These proteins-STOM, GTR1, ACTN1, MAGT1, STML3, AKAP13, and CAMP3-are novel candidates that are up-regulated not only in the PMA-treated HCC cell line, but also in other cancers originating from different cell types [27-32]. STOM is over expressed in cancer and is involved in regulating cell growth [33]. GTR1 facilitates glucose transportation and maintains basal glucose uptake [34], and is highly expressed in cancer cells to fulfill their energy requirements for survival and metastasis [27, 35]. ACTN1 has a close association with cellular membranes and forms a complex with diacylglycerol and fatty acid [36]. The interaction between the cytoskeleton and membrane may participate in the regulation of cell function through changes in cell shape and cellular migration [37]. Moreover, the up-regulation of α-actinin in invading HCC cells in our study is consistent with data from Nishiyama *et al.,* who observed higher transcription levels of *ACTN1* mRNA in HCC tissue compared with non-involved adjacent tissue [37]. MAGT1 is universally expressed in all human tissues and its expression level is up regulated in conditions of low extracellular Mg^{2+} [38]. STML3 is a domain protein of prohibitin (PHB) that is inserted into the membrane through an intramembrane domain resulting in hairpin-like topology with both the N- and C-termini facing the cytoplasm, [39] and is associated with cellular membrane processes such as ion channel regulation, membrane protein chaperoning, vesicle and protein trafficking, membrane-cytoskeletal coupling, microdomain formation, and the formation of specialized membrane structures. AKAP13 (also known as lymphoid blast crisis oncogene [LBC]) is absent in normal adult liver but abundantly expressed in HCC [40]. CAMP3 accumulates along cell junctions and plays a key role in maintaining a population of noncentrosomal microtubules that is important for proper organelle assembly [32].

All seven cytoplasmic membrane candidates were initially validated by semi-quantitative real-time RT-PCR. The results showed that *MAGT1* and *AKAP13* were predominantly up-regulated in PMA-treated HepG2 cells but, surprisingly, the other five candidates (*STOM*,

GTR1, *ACTN1*, *STML3*, and *CAMP3*) showed a decrease in transcription levels that was not consistent with the level of protein expression from mass spectrometry. This may be caused by post-transcriptional regulatory processes, such as miRNA [41], protein stability [42], or protein degradation [43], that inhibit translational processes in non-treated HCC cells. Down-regulation of the miRNA200 family was observed in the invasive front of colorectal adenocarcinoma but not in non-invasive and normal cells [44] and might reflect inhibition of E-cadherin expression through increased expression of ZEB protein (a E-cadherin repressor) [45]. Similarly, lack of miRNA200 and E-cadherin may influence cancer invasion in metastatic human breast cancer [46]. However, the controversial results of the five different candidates mentioned above occurred through unknown mechanisms and require further exploration.

Our results showed that MAGT1 and AKAP13 were predominantly expressed in response to PMA at both mRNA and protein levels. Therefore, both proteins were selected for further validation in *in vitro* and clinical HCC samples. MAGT1 has been demonstrated to be essential for vertebrate Mg^{2+} influx [47]. It is universally expressed in all human tissues and its expression level is up-regulated in conditions of low extracellular Mg^{2+} [38]. Mg^{2+} is the second most common cation in intracellular fluids. Appropriate Mg^{2+} levels have been shown to be involved in physiological functions such as nucleic acid metabolism, protein synthesis, and energy production [48, 49]. Interestingly, it has recently been proposed that Mg^{2+} might also initiate cell proliferation upon mitogenic stimulus because cells are able to increase their intracellular Mg^{2+} content, which is needed for initiation of protein synthesis, by activating Mg^{2+} influx [50, 51]. Therefore, influx of both extracellular Ca^{2+} and Mg^{2+} must be tightly maintained for proper intracellular ion homeostasis. Furthermore, alterations in this homeostasis will likely increase cell proliferation and can lead to cancer [52]. However, the role of MAGT1 in cancer is still unclear.

AKAP13 is an anchoring protein in the Rho signaling pathway that is abundantly expressed in HCC but not in normal adult liver [40]. Over expression of AKAP13 in HCC cell lines promoted cell proliferation and triggered high levels of downstream ERK and cyclin D1 [40]. Hu and colleagues reported that the expression of AKAP13 in colorectal carcinoma was higher than that in normal colorectal tissues and adenoma, indicating that AKAP13 might play a role in the carcinogenesis of colorectal carcinoma. This would be consistent with the proposed function of the PKA/AKAP13/RhoA signaling pathway in the proliferation and differentiation of many human cancers [53]. AKAP13 is also known as lymphoid blast crisis oncogene. It is capable of both anchoring PKA and activating Rho GTPases and is an important upstream effector of RhoA, catalyzing the GDP-GTP exchange reaction required for RhoA signaling [54, 55]. Rho protein is also involved in invasion and metastasis. It has been demonstrated that the PKA/AKAP13/RhoA signaling pathway plays an important role in carcinogenesis and tumor development [56-58]. Some studies have reported mutation of the *AKAP*13 gene in familial breast cancer and proposed a relationship between AKAP13 and prostatic cancer [31, 59, 60]. However, the role of AKAP13 in hepatocellular carcinoma invasion and metaplasia has not been described.

Western blot analysis yielded the same results as mass spectrophotometry and SYBR real time RT-PCR, confirming up-regulation of MAGT1 and AKAP13 during HCC cell invasion. Expression of MAGT1 and AKAP13 in HepG2 cells was highest 24 h after PMA induction, but decreased with prolonged incubation of 48 h. Reduction of protein expression at 48 h may be due to cell arrest induced by starvation under serum-depleted conditions [61, 62]. Immunofluorescent staining suggested that both MAGT1 and AKAP13 were localized at cytoplasmic membranes and in perimembranous areas. The same location of MAGT1 and AKAP13 has been reported in normal cells and other cancers expressing invasiveness and metaplasia [31, 38, 59, 60]. This may imply a function in facilitating cancer invasion and migration. However, the exact association of MAGT1 and AKAP13 with metaplastic characteristics requires intensive characterization in future studies.

Detection of protein expression in clinical HCC tissues revealed a strong cytoplasmic staining pattern in tumoral tissues but no or weak

expression in non-tumoral surrounding tissues. Expression of MAGT1 and AKAP13 in clinical HCC tissues may support a potential role of these proteins as novel prognostic and/or diagnostic markers. However, validation of these findings in more clinical HCC tissues at different stages and distinct cancer types is needed. In conclusion, high expression levels of MAGT1 and AKAP13 at the cytoplasmic membrane and in the cytoplasm of an invasive HCC cell line and clinical samples of invasive and progressive HCC suggest potential for the development of novel HCC markers to improve prognosis, diagnosis, and treatment management for HCC in the future.

Acknowledgements

This work was partially supported by the National Research Universities (NRU) and NSTDA Chair Professor 2013 Scholarships through Professor Wanpen Chaicumpa, Department of Parasitology, Faculty of Medicine Siriraj Hospital, Mahidol University, Bangkok, Thailand. We thank Professor Sanya Sukpanichnant, Department of Pathology, Faculty of Medicine Siriraj Hospital, Mahidol University Bangkok, Thailand for valuable suggestions regarding immunohistochemistry. Our gratitude goes to the Faculty of Tropical Medicine, Mahidol University for funding the proofreading and correcting this manuscript.

Disclosure of conflict of interest

None.

Address correspondence to: Dr. Urai Chaisri, Department of Tropical Pathology, Faculty of Tropical Medicine, Mahidol University, 420/6 Rajvithi Road, Bangkok 10400, Thailand. Tel: (66)-2306-9184; Fax: (66)-2306-9184; E-mail: urai.cha@mahidol.ac.th

References

[1] Cheng P, Cheng Y, Su MX, Li D, Zhao GZ, Gao H, Li Y, Zhu JY, Li H and Zhang T. Bicluster and pathway enrichment analysis of HCV-induced cirrhosis and hepatocellular carcinoma. Asian Pac J Cancer Prev 2012; 13: 3741-3745.

[2] Jemal A, Bray F, Center MM, Ferlay J, Ward E and Forman D. Global cancer statistics. CA Cancer J Clin 2011; 61: 69-90.

[3] El-Serag HB and Rudolph KL. Hepatocellular carcinoma: epidemiology and molecular carcinogenesis. Gastroenterology 2007; 132: 2557-2576.

[4] Farinati F, Marino D, De Giorgio M, Baldan A, Cantarini M, Cursaro C, Rapaccini G, Del Poggio P, Di Nolfo MA, Benvegnu L, Zoli M, Borzio F, Bernardi M and Trevisani F. Diagnostic and prognostic role of alpha-fetoprotein in hepatocellular carcinoma: both or neither? Am J Gastroenterol 2006; 101: 524-532.

[5] Trinchet JC, Chaffaut C, Bourcier V, Degos F, Henrion J, Fontaine H, Roulot D, Mallat A, Hillaire S, Cales P, Ollivier I, Vinel JP, Mathurin P, Bronowicki JP, Vilgrain V, N'Kontchou G, Beaugrand M and Chevret S. Ultrasonographic surveillance of hepatocellular carcinoma in cirrhosis: a randomized trial comparing 3- and 6-month periodicities. Hepatology 2011; 54: 1987-1997.

[6] Lund R, Leth-Larsen R, Jensen ON and Ditzel HJ. Efficient Isolation and Quantitative Proteomic Analysis of Cancer Cell Plasma Membrane Proteins for Identification of Metastasis-Associated Cell Surface Markers. J Proteome Res 2009; 8: 3078-3090.

[7] Ziegler YS, Moresco JJ, Tu PG, Yates JR 3rd and Nardulli AM. Plasma Membrane Proteomics of Human Breast Cancer Cell Lines Identifies Potential Targets for Breast Cancer Diagnosis and Treatment. PLoS One 2014; 9: e102341.

[8] Kaufmann R, Müller P, Hildenbrand G, Hausmann M and Cremer C. Analysis of Her2/neu membrane protein clusters in different types of breast cancer cells using localization microscopy. J Microsc 2011; 242: 46-54.

[9] Chiang SF, Tsai MH, Tang R, Hsieh LL, Chiang JM, Yeh CY, Hsieh PS, Tsai WS, Liu YP, Liang Y, Chen JS and Yu JS. Membrane Proteins as Potential Colon Cancer Biomarkers: Verification of 4 Candidates from a Secretome Dataset. Surg Sci 2014; 10: 21.

[10] Yang G, Goltsov AA, Ren C, Kurosaka S, Edamura K, Logothetis R, DeMayo FJ, Troncoso P, Blando J, DiGiovanni J and Thompson TC. Caveolin-1 Upregulation Contributes to c-Myc–Induced High-Grade Prostatic Intraepithelial Neoplasia and Prostate Cancer. Mol Cancer Res 2012; 10: 218-229.

[11] Bozkaya G, Korhan P, Cokakli M, Erdal E, Sagol O, Karademir S, Korch C and Atabey N. Cooperative interaction of MUC1 with the HGF/c-Met pathway during hepatocarcinogenesis. Mol Cancer 2012; 11: 64.

[12] Filmus J and Selleck SB. Glypicans: proteoglycans with a surprise. J Clin Invest 2001; 108: 497-501.

[13] Sung YK, Hwang SY, Park MK, Farooq M, Han IS, Bae HI, Kim JC and Kim M. Glypican-3 is overexpressed in human hepatocellular carcinoma. Cancer Sci 2003; 94: 259-262.

[14] Cho HJ, Kang JH, Kwak JY, Lee TS, Lee IS, Park NG, Nakajima H, Magae J and Chang YC. Ascofuranone suppresses PMA-mediated matrix metalloproteinase-9 gene activation through the Ras/Raf/MEK/ERK- and Ap1-dependent mechanisms. Carcinogenesis 2007; 28: 1104-1110.

[15] Liu P, Kimmoun E, Legrand A, Sauvanet A, Degott C, Lardeux B and Bernuau D. Activation of NF-kappa B, AP-1 and STAT transcription factors is a frequent and early event in human hepatocellular carcinomas. J Hepatol 2002; 37: 63-71.

[16] Weng CJ, Chau CF, Hsieh YS, Yang SF and Yen GC. Lucidenic acid inhibits PMA-induced invasion of human hepatoma cells through inactivating MAPK/ERK signal transduction pathway and reducing binding activities of NF-kappaB and AP-1. Carcinogenesis 2008; 29: 147-156.

[17] Stockert JC, Blázquez-Castro A, Cañete M, Horobin RW and Villanueva Á. MTT assay for cell viability: Intracellular localization of the formazan product is in lipid droplets. Acta Histochem 2012; 114: 785-796.

[18] Marshall J. Transwell® Invasion Assays. In: Wells CM, Parsons M, editors. Cell Migration. Humana Press; 2011. pp. 97-110.

[19] Adisakwattana P, Suwandittakul N, Petmitr S, Wongkham S, Sangvanich P and Reamtong O. ALCAM is a Novel Cytoplasmic Membrane Protein in TNF-alpha Stimulated Invasive Cholangiocarcinoma Cells. Asian Pac J Cancer Prev 2015; 16: 3849-3856.

[20] Ishihama Y, Oda Y, Tabata T, Sato T, Nagasu T, Rappsilber J and Mann M. Exponentially modified protein abundance index (emPAI) for estimation of absolute protein amount in proteomics by the number of sequenced peptides per protein. Mol Cell Proteomics 2005; 4: 1265-1272.

[21] Pfaffl MW. Relative quantification. Real-time PCR 2006; 63-82.

[22] Ramos-Vara JA. Principles and methods of immunohistochemistry. Methods Mol Biol 2011; 691: 83-96.

[23] Kaemmerer D, Peter L, Lupp A, Schulz S, Sanger J, Baum RP, Prasad V and Hommann M. Comparing of IRS and Her2 as immunohistochemical scoring schemes in gastroenteropancreatic neuroendocrine tumors. Int J Clin Exp Pathol 2012; 5: 187-194.

[24] Chen CJ and Lee MH. Early Diagnosis of Hepatocellular Carcinoma by Multiple microRNAs: Validity, Efficacy, and Cost-Effectiveness. J Clin Oncol 2011; 29: 4745-4747.

[25] Bialecki ES and Di Bisceglie AM. Diagnosis of hepatocellular carcinoma. HPB (Oxford) 2005; 7: 26-34.

[26] Hwang YP, Yun HJ, Kim HG, Han EH, Lee GW and Jeong HG. Suppression of PMA-induced tumor cell invasion by dihydroartemisinin via inhibition of PKCalpha/Raf/MAPKs and NF-kappaB/AP-1-dependent mechanisms. Biochem Pharmacol 2010; 79: 1714-1726.

[27] Vander Heiden MG, Cantley LC and Thompson CB. Understanding the Warburg Effect: The Metabolic Requirements of Cell Proliferation. Science 2009; 324: 1029-1033.

[28] Arkhipova KA, Sheyderman AN, Laktionov KK, Mochalnikova VV and Zborovskaya IB. Simultaneous expression of flotillin-1, flotillin-2, stomatin and caveolin-1 in non-small cell lung cancer and soft tissue sarcomas. BMC Cancer 2014; 14: 100.

[29] Craig DH, Haimovich B and Basson MD. α-Actinin-1 phosphorylation modulates pressure-induced colon cancer cell adhesion through regulation of focal adhesion kinase-Src interaction. Am J Physiol Cell Physiol 2007; 293: C1862-74.

[30] Green J and Young JP. Slipins: ancient origin, duplication and diversification of the stomatin protein family. BMC Evol Biol 2008; 8: 44.

[31] Wirtenberger M, Schmutzhard J, Hemminki K, Meindl A, Sutter C, Schmutzler RK, Wappenschmidt B, Kiechle M, Arnold N, Weber BH, Niederacher D, Bartram CR and Burwinkel B. The functional genetic variant Ile646Val located in the kinase binding domain of the A-kinase anchoring protein 10 is associated with familial breast cancer. Carcinogenesis 2007; 28: 423-426.

[32] Tanaka N, Meng W, Nagae S and Takeichi M. Nezha/CAMSAP3 and CAMSAP2 cooperate in epithelial-specific organization of noncentrosomal microtubules. Proc Natl Acad Sci U S A 2012; 109: 20029-20034.

[33] Zhang L, Ding F, Cao W, Liu Z, Liu W, Yu Z, Wu Y, Li W and Li Y. Stomatin-like protein 2 is overexpressed in cancer and involved in regulating cell growth and cell adhesion in human esophageal squamous cell carcinoma. Clin Cancer Res 2006; 12: 1639-1646.

[34] Macheda ML, Rogers S and Best JD. Molecular and cellular regulation of glucose transporter (GLUT) proteins in cancer. J Cell Physiol 2005; 202: 654-662.

[35] Kim JW and Dang CV. Cancer's molecular sweet tooth and the Warburg effect. Cancer Res 2006; 66: 8927-8930.

[36] Burn P, Rotman A, Meyer RK and Burger MM. Diacylglycerol in large [alpha]-actinin/actin complexes and in the cytoskeleton of activated platelets. Nature 1985; 314: 469-472.

[37] Nishiyama M, Ozturk M, Frohlich M, Mafune K, Steele G Jr and Wands JR. Expression of hu-

man alpha-actinin in human hepatocellular carcinoma. Cancer Res 1990; 50: 6291-6294.
[38] Zhou H and Clapham DE. Mammalian MagT1 and TUSC3 are required for cellular magnesium uptake and vertebrate embryonic development. Proc Natl Acad Sci U S A 2009; 106: 15750-15755.
[39] Browman DT, Hoegg MB and Robbins SM. The SPFH domain-containing proteins: more than lipid raft markers. Trends Cell Biol 2007; 17: 394-402.
[40] Sterpetti P, Marucci L, Candelaresi C, Toksoz D, Alpini G, Ugili L, Baroni GS, Macarri G and Benedetti A. Cell proliferation and drug resistance in hepatocellular carcinoma are modulated by Rho GTPase signals. Am J Physiol Gastrointest Liver Physiol 2006; 290: G624-632.
[41] Valinezhad Orang A, Safaralizadeh R and Kazemzadeh-Bavili M. Mechanisms of miRNA-Mediated Gene Regulation from Common Downregulation to mRNA-Specific Upregulation. Int J Genomics 2014; 2014: 970607.
[42] Lerner LE, Piri N and Farber DB. Transcriptional and post-transcriptional regulation of the rod cGMP-phospho diesterase beta-subunit gene. Recent advances and current concepts. Adv Exp Med Biol 2006; 572: 217-229.
[43] Vogel C and Marcotte EM. Insights into the regulation of protein abundance from proteomic and transcriptomic analyses. Nat Rev Genet 2012; 13: 227-232.
[44] Paterson EL, Kazenwadel J, Bert AG, Khew-Goodall Y, Ruszkiewicz A and Goodall GJ. Down-Regulation of the miRNA-200 Family at the Invasive Front of Colorectal Cancers with Degraded Basement Membrane Indicates EMT Is Involved in Cancer Progression. Neoplasia (New York, N.Y.) 2013; 15: 180-191.
[45] Korpal M, Lee ES, Hu G and Kang Y. The miR-200 Family Inhibits Epithelial-Mesenchymal Transition and Cancer Cell Migration by Direct Targeting of E-cadherin Transcriptional Repressors ZEB1 and ZEB2. J Biol Chem 2008; 283: 14910-14914.
[46] Hilmarsdottir B, Briem E, Bergthorsson JT, Magnusson MK and Gudjonsson T. Functional Role of the microRNA-200 Family in Breast Morphogenesis and Neoplasia. Genes (Basel) 2014; 5: 804-820.
[47] Quamme GA. Molecular identification of ancient and modern mammalian magnesium transporters. Am J Physiol Cell Physiol 2010; 298: C407-429.
[48] Hazelton B, Mitchell B and Tupper J. Calcium, magnesium, and growth control in the WI-38 human fibroblast cell. J Cell Biol 1979; 83: 487-498.
[49] Anghileri LJ. Magnesium, calcium and cancer. Magnes Res 2009; 22: 247-255.
[50] Wolf FI, Fasanella S, Tedesco B, Torsello A, Sgambato A, Faraglia B, Palozza P, Boninsegna A and Cittadini A. Regulation of magnesium content during proliferation of mammary epithelial cells (HC-11). Front Biosci 2004; 9: 2056-2062.
[51] Rubin H. Central roles of Mg2+ and MgATP2- in the regulation of protein synthesis and cell proliferation: significance for neoplastic transformation. Adv Cancer Res 2005; 93: 1-58.
[52] Sun Y, Selvaraj S, Varma A, Derry S, Sahmoun AE and Singh BB. Increase in serum Ca2+/Mg2+ ratio promotes proliferation of prostate cancer cells by activating TRPM7 channels. J Biol Chem 2013; 288: 255-263.
[53] Hu JK, Wang L, Li Y, Yang K, Zhang P, Chen XZ, Wang R and Zhou ZG. The mRNA and protein expression of A-kinase anchor proteins 13 in human colorectal cancer. Clin Exp Med 2010; 10: 41-49.
[54] Diviani D, Abuin L, Cotecchia S and Pansier L. Anchoring of both PKA and 14-3-3 inhibits the Rho-GEF activity of the AKAP-Lbc signaling complex. EMBO J 2004; 23: 2811-2820.
[55] Diviani D, Soderling J and Scott JD. AKAP-Lbc anchors protein kinase A and nucleates Galpha 12-selective Rho-mediated stress fiber formation. J Biol Chem 2001; 276: 44247-44257.
[56] Sahai E and Marshall CJ. RHO-GTPases and cancer. Nat Rev Cancer 2002; 2: 133-142.
[57] Etienne-Manneville S and Hall A. Rho GTPases in cell biology. Nature 2002; 420: 629-635.
[58] Carnegie GK, Means CK and Scott JD. A-kinase anchoring proteins: from protein complexes to physiology and disease. IUBMB Life 2009; 61: 394-406.
[59] Wirtenberger M, Tchatchou S, Hemminki K, Klaes R, Schmutzler RK, Bermejo JL, Chen B, Wappenschmidt B, Meindl A, Bartram CR and Burwinkel B. Association of genetic variants in the Rho guanine nucleotide exchange factor AKAP13 with familial breast cancer. Carcinogenesis 2006; 27: 593-598.
[60] Lewis TE, Milam TD, Klingler DW, Rao PS, Jaggi M, Smith DJ, Hemstreet GP and Balaji KC. Tissue transglutaminase interacts with protein kinase A anchor protein 13 in prostate cancer. Urol Oncol 2005; 23: 407-412.
[61] Pirkmajer S and Chibalin AV. Serum starvation: caveat emptor. Am J Physiol Cell Physiol 2011; 301: C272-9.
[62] Lin SP, Lee YT, Wang JY, Miller SA, Chiou SH, Hung MC and Hung SC. Survival of Cancer Stem Cells under Hypoxia and Serum Depletion via Decrease in PP2A Activity and Activation of p38-MAPKAPK2-Hsp27. PLoS One 2012; 7: e49605.